

Network deployment for Energy Efficiency using Single-Slope and Multiple-Slope Path Loss Models

¹Ritu Singh Phogat, ²Dr. Rutvij Joshi

¹*Electronics and Communication, Gujarat Technological University, Gujarat, India*

²*Electronics and Communication, Parul University, Gujarat, India*

Abstract: The majority of resource allocation methods used today in cell service are found on the single-slope path loss prototype, which does not adequately account for the influence of the physical environment. Cell patterns become more erratic due to the phenomenon of densification, therefore the multi-slope model is more accurate in approximating the expanded variances in the linkages and intervention. The uplink (UL) of a cell network is being delineated in this study to be as energy-efficient as possible. Every base station (BS), which is arbitrarily distributed throughout a region, is furnished with M antennas to accommodate K user gadgets. With the understanding that pilot sequences are utilised to gather channel state information, a multi-slope or distance dependent path loss framework is considered. In this situation, the network EE is assessed using a practical circuit power utilization prototype and a lower bound on the uplink SE. The best base station solidity and pilot reuse component for a Massive MIMO web with alternative plots—maximum ratio combining, zero-forcing, and multicell minimal mean-squared error—are first calculated using numerical calculations. No matter the detection method used, the parametric investigation demonstrates that the energy efficiency is a single mode assignment of base station solidity and reaches its paramount for a corresponding low BS density. The energy efficiency is a monotonous non-deductable assignment of BS solidity in the distance independent path loss prototype, in contrast.

Keywords: Energy Efficiency, Massive MIMO, Single slope model, Multi-slope model

I. Introduction

Network densification has attained a lot of interest in the 5G webworks in order to control the wireless data traffic's exponential increase and enable high data rates [1],[2].

A crucial issue is how to advance connection automations to give greater throughput beyond unreasonably raising power utilization[3]. This necessitates the development of innovative design strategies that offer user equipment (UEs) great spectrum efficiency at reasonable energy prices. There is general agreement that significant network densification is required to achieve this wireless capacity expansion.[4],[5]. Two primary methods for achieving this cram are small-cell web [6][7][8] and massive MIMO. [9][10][11]. The preceding depends on a wide-scale tiny cell deployment that ensures bottommost propagation dropping. Through the usage of spatial multiplexing, the latter employs an enormous quantity of base station antennas to concurrently service a sizable quantity of UEs. In the research literature, there has also been a lot of interest in a combination of both. Despite having the potential to improve SE, twain options seems to grow the amount of power used by the network, massive MIMO needs additional equipments per BS, whilst tiny cells expand the quantity of distributed BSs. The goal of this effort is to create a cellular network from the ground up with the highest energy efficiency possible without making any presumptions about the quantity of base station antennas, user ends, pilot reuse, or base station solidity in advance.

II. Literature Survey

In the literature, there has been a lot of discussion over how to deploy cellular networks most effectively. The Wyner model places twain BSs and UEs on a line at defined locations. [12]. The consideration of more advanced two dimensional mirrored grid-based distribution, such as honeycomb, followed [13]. Twain methods are unsuitable for investigating and modelling networks with a very erratic and thick framework, such as those found in coming cellular networks. In recent years, sophisticated mathematical techniques built on stochastic topology have been applied to this problem [14],[15]. The positions of BSs in the stochastic geometry framework constitute a point process in a diminutive group whose centroid is an independent Poisson dispersed arbitrary component over several disjoint sets. There are numerous measures to gauge a cellular network's performance, including throughput, EE, and coverage likelihood[7]. In [7], [16], and [17], stochastic geometry is employed to construct the EE analysis of a multicell network. According to [16], the optimization is carried out while meeting UE-specific quality-of-service requirements. The usage of small-cells in conjunction with resting techniques has

been shown in [7] and [17] to be an intriguing method for boosting the energy efficiency. In general, small-cells result in a greater energy efficiency, but this advantage swiftly reaches saturation as the solidity of small cells rises. Massive MIMO has been demonstrated in [18] to have other advantages. All of the aforementioned publications, like the most of works in the writings, employ the common path loss framework, where accepted energy declines as $d^{-\alpha}$ over a proximity d , where α is referred to as the "path loss exponent." In a real-world setting, it would be simple to distinguish between three different regimes. [19]. $\alpha_0 = 0$ in the distance-independent "nearfield," $\alpha_1 = 2$ in the free-space-like regime, and $\alpha_2 > 2$ in the greatly attenuated domain. Identification of the network functioning pattern for which a rise, engorgement, or decay of the production is seen when the network gentrify depends critically on the propagation domain and dissolving dispersion. Ultra BS-densification may possibly result in nil throughput in the worst-case scenario. Despite this, multislope framework are rarely employed in the study of cell web since they typically increase the difficulty of the conceptual study. For the given EE maximisation problem, this paper makes an attempt to resolve this challenge.

III. Contribution

In this case, the analogous Poisson point process (H-PPP) of potency is used to distribute the BSs separately and evenly across a provided area in a cellular network. Every BS has an arbitrary number M of antennas and can support up to K UEs at once. In the uplink (UL), empirical channel convergence power-management is utilized to ensure a constant average signal to noise ratio (SNR) along all UEs. Considered is a multislope framework. Under the presumption that CSI is obtained by utilising pilots, which are repeated throughout the network with a component ζ , divergent linear combining structures—maximum ratio (MR), zero-forcing (ZF), and multicell minimum mean-squared error (M-MMSE)—are utilised. The network's EE is calculated using a polynomial power consumption model that was extensively researched in [20], a lower bound on the average uplink SE, and any combining strategy. As a result of the findings, it can be seen that the energy efficiency with a multislope is a single mode function of BS Density (λ). The best EE is attained for slightly low virtues of λ and ζ , regardless of the detecting strategy used. This is in stark contrast to [18], which establishes that densification is always advantageous for EE by usage of a single-slope framework in [18], the energy efficiency is demonstrated to be a monotonically rising function of λ . The findings also demonstrate that when BS density rises, the three distinct methods act identically reference to energy efficiency and area throughput, even though the "ideal" M-MMSE combiner offers the best EE.

In comparison to the draught edition in [21], this exertion: (i) gives the EE insight for MR, ZF, and M-MMSE (ii) is designed on a multislope path loss framework and seeks to demonstrate how it affects energy efficiency when the network is thick and (iii) provides additional information and clarity into the impact of web specifications and circuit energy framework.

IV. Network Framework and Issue Description

The uplink of a cell web in which the base stations are dispersed dimensionally is analysed. As per H-PPP, $\{x_i\} \in \mathbb{R}^2$ within a small geographic area equals $\Phi_\lambda = \{x_i; i \in \mathbb{N}\}$ of concentration λ [BS/km²]. The regular quantity of distributed BSs is λA , assuming that A is the deployment area of interest. In a bandwidth of B_w [MHz], each BS serves K single-antenna user ends using M antennas. Using some scheduling technique, these K UEs are chosen arbitrarily from a huge group. Each UE is considered to be connected to the nearest BS, and as a result, each BS's coverage area is represented by a Poisson-Voronoi cell (Figure 1). Synchronous time-division-duplex protocol governs how the network functions. The coherence bandwidth and time are indicated by B_c [Hz] and T_c [s], respectively. $\tau_c = B_c T_c$ is coherence block. τ_p samples are utilised in each coherence block to gather channel state data via uplink pilot sequences, while τ_u and τ_d samples are used to transmit payload in the uplink and downlink (DL), respectively. The uplink payload signal sent from user end i of cell l to its serving base station l with energy $p_{li} = E_s\{|s_{li}|\}^2$ is referred to as $s_{li} \mathcal{N}_C(0, p_{li})$. $y_j \in \mathbb{C}^M$ is the signal that BS j has received and is given as:

$$y_j = h_{jk}^j s_{jk} + \sum_{i=1, i \neq k}^K h_{ji}^j s_{ji} + \sum_{l \in \Phi_{\lambda(j)}} \sum_{i=1}^K h_{li}^j s_{li} + n_j \quad (1)$$

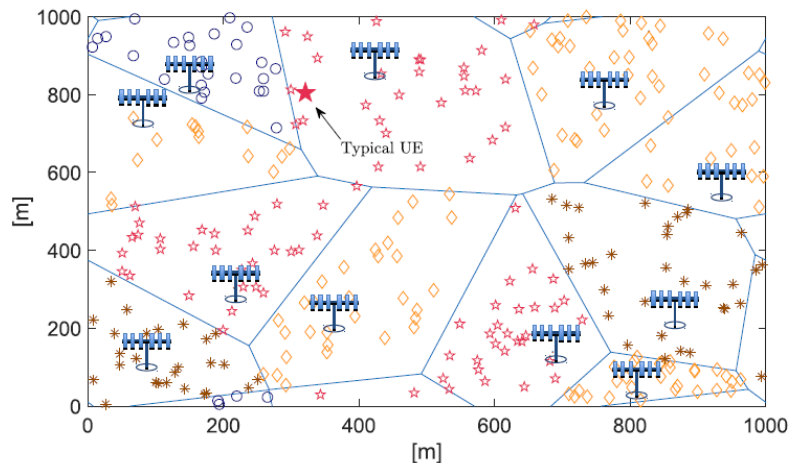


Fig 1: cellular network deployment using BSs sourced from an H-PPP. Cell j's typical UE k is highlighted. The same marking and colour are used to represent the user end of several cells that portion the same pilot section.

Where $n_j \sim \mathcal{NC}(0, \sigma^2 I_M)$ is the additive Gaussian noise, $h_{li}^j \in CM$ is the channel response amid user end i in cell l and base station j customized as uncorrelated Rayleigh fading. d_{li}^j the distance of user end i in cell l from base station j and compute β_{li}^j as per general multislope path loss framework, which is expressed as:

$$\beta_{li}^j = \Upsilon_n (d_{li}^j)^{-\alpha_n} \tag{2}$$

With $d_{li}^j \in [R_{n-1}, R_n]$ [km], for $n = 1, \dots, N$. The coefficients $\{\Upsilon_n\}$, $\{\alpha_n\}$ are design parameters.

Specifically, $0 \leq \alpha_1 \leq \dots \leq \alpha_N$ are the energy decline components, $0 = R_0 < \dots < R_N = \infty$ designate the range at which a alteration in the power declination takes place. Keeping $N=1$ gives single slope framework. It is assumed the user ends use the empirical channel inversion power-management structure such that $p_{li} = P_0 / \beta_{li}^j$ where P_0 is a design parameter. It is assumed that in every coherence fragment, each base station l selects a section of K distinct patterns from Φ , evenly at random, and distributes them amid its serviced user ends in order to avoid onerous pilot coordination.

V. Analysis Of Energy Efficiency

The definition of the EE, which is mathematically represented as “the amount of information that can be reliably conveyed per unit of energy,” is

$$EE = \frac{\text{Area Throughput}}{\text{Area Power Consumption}} = \frac{B_w \cdot ASE}{APC} \tag{3}$$

Which can be viewed as benefit cost proportion. ASE and APC represents the area spectral efficiency (ASE) and area power consumption (APC), respectively.

$$ASE = \lambda k SE \text{ (average uplink se of the typical user end k in cell j)}$$

The term SE stands for the typical UE k's average UL spectral efficiency in cell j, which is calculated by averaging over various user end locations, pilot allotment, and channel realisations. The multiplicative component K, which equals the BS density per km², allows for the total spectral efficiency of all user ends in cell j and λ .

A lower bound on SE, which holds for any combining scheme is

$$SE = \xi \left(1 - \frac{K\zeta}{\tau_c}\right) \mathbb{E}_{\{d,h,a\}} \{\log_2(1 + SINR')\}$$
(4)

where $SINR'$ is instantaneous SINR

$$SINR' = \frac{p_{jk} |V_{jk}^H \hat{h}_{jk}^j|^2}{V_{jK}^H \left(\sum_{l \in \Phi_\lambda} \sum_{\substack{i=1 \\ (l,i) \neq (j,k)}}^K p_{li} \hat{h}_{li}^j \hat{h}_{li}^{jH} + \sum_{l \in \Phi_\lambda} \sum_{i=1}^K P_{li} (\beta_{li}^j - \gamma_{li}^j) I_M + \sigma^2 I_M \right) V_{jk}}$$
(5)

With regard to user end locations, channel realisations, and pilot allotment, the expectation $\mathbb{E}_{\{d,h,a\}}$ is calculated. Pilot overhead is taken into consideration via the pre-log factor.

VI. Power Model

The APC is formally defined as

$$APC = \lambda(\eta^{-1} P_{TX} + P_{CP})$$
(6)

where $\eta \in (0,1]$ is the high energy amplifier (HPA) efficiency and P_{TX} represents the typical power used for uplink transmission (payload and pilots) in an random cell j . P_{CP} represents the power used by the circuitry and can be calculated as in [18], [22].

$$P_{TX} = \left(\frac{\tau_u + \rho\tau_p}{\tau_c}\right) K\mathcal{U}$$
(7)

where \mathcal{U} is power per user of multislope path loss model. The amount of power required to run any given BS is modelled as

$$P_{CP} = P_{FIX} + P_{TC} + P_{C-BH} + P_{CE} + P_{LP}$$
(8)

where P_{TC} stands for the transceiver chain, P_{FIX} is the energy used for location cool down, managing signalling, and load-independent retrieval of data, P_{CBH} is the cost of coding and load-dependent retrieval of data, P_{CE} is the channel prediction procedure, and P_{LP} is the linear sequencing.

Steps of Algorithm to compute single slope and multi slope path loss model

- Compute the lower bound on the median ergodic SE as shown above.
- The UEs and the BSs randomly within the coverage area are deployed.
- Compute all the uplink channel estimate for all UEs in the entire networks
- Compute the average channel gain of the channel between UEs at random locations and the BSs
- Retrieve the quantity of user end K and the quantity of slopes in the multi-slope Model
- Compute the large-scale fading coefficients (assign path-loss exponent according to the distances BS
- Calculate the total Consumed Power with different processing schemes.
- Single slope Pathloss Model
- Load SE simulation data related to the single slope path loss framework [18].
- Retrieve the SNRs value in dB in the inverse statistical power control policy
 - $SNR = 10^{(\Delta dB/10)}$;
 - $SNR_p = 10^{(\Delta dB_{pilot}/10)}$
 - Compute UL sum SE using the fractions of UL data [18]
 - Go through all number of BS densities and all number of Pilot reuse factors
- Compute the total CP with different schemes
- Compute EE of all schemes

- **Multislope Path loss Model**
 - Load SE simulation data related to the multislope path loss model
 - Repeat all steps similar to single slope model
- **Output**
 - Multislope EE v/s Singleslope EE as a function of Base Station Density

VII. Numerical Analysis

These parameters frequently take on significantly different values because of how strongly hardware-specific they are.

Table 1: Network and System specifications

Parameter	Value	Parameter	Value
Fixed power: P_{FIX}	5 W	Far-field path loss exponent: α	4
Power for BS Local Oscillator: P_{LO}	0.1W	Coherence block length: τ_c	200 samples
Power per BS antennas: P_{BS}	0.2W	Propagation loss at 1 km: γ	-148.1 dB
Power for antenna at UE: P_{UE}	0.1W	Bandwidth: B_w	20Mhz
Power for data coding: P_{COD}	0.01W/(Gbit/s)	Deployment area: A	1 km ²
Power for backhaul traffic: P_{BT}	0.025W/(Gbit/s)	UL fraction of payload block: ξ	1/3
Power for data decoding: P_{DEC}	0.08W/(Gbit/s)	Noise variance: σ^2	-94 dBm
BS computational efficiency: L_{BS}	750 Gflops/W	Signal-to-noise ratio of payload block: SNR_0	5 dB
HPA efficiency: η	0.5	Signal-to-noise ratio of pilot block: SNR_p	15 dB

We take into account a deployment area of $A = 1 \text{ km}^2$, where $E\{\Phi_\lambda\} = \lambda A$ BSs are dispersed at random in accordance with an H-PPP. To imitate the H-PPP in the entire R^2 and maintain transferral variability, a wrap-around topology is employed.

For the large scale fading in (2), a bounded $N = 3$ sloping path loss framework is employed with parameters $[\alpha_1, \alpha_2, \alpha_3] = [0, 2, \alpha]$, $[R_1, R_2] = [10, 446] \text{ [m]}$, and $[\gamma_1, \gamma_2, \gamma_3] = [1, 1, \gamma]$ with γ and α as in Table 1. This model was inspired by [23] and [24]. In order to meet the channel hardening and advantageous propagation circumstances, a Massive MIMO system is taken into consideration, which is approximately characterised by an antenna-user end ratio $M/K = 10$ [20]. $M = 100$ and $K = 10$ is used in this setup.

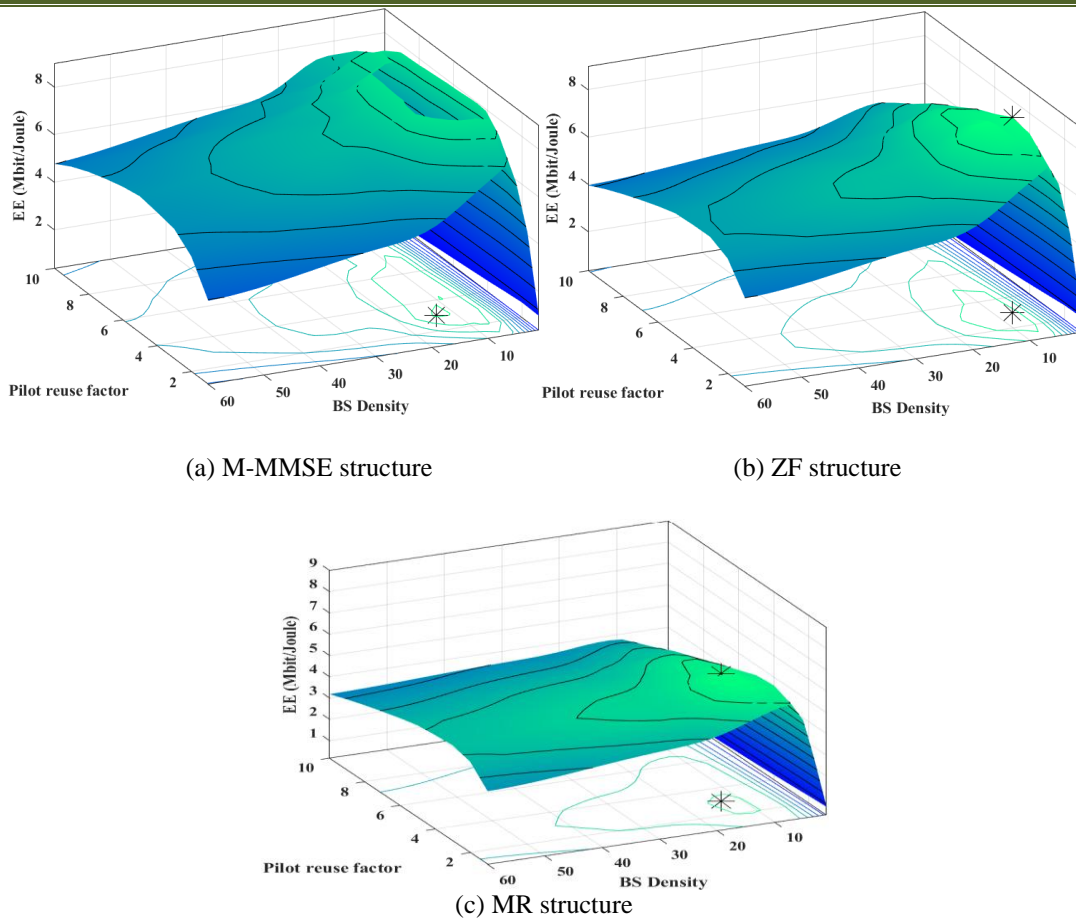


Fig. 2: EE as assignment of λ and ζ . Results are obtained by Monte Carlo simulations within Massive MIMO framework.

The EE-optimum network dispersal layout for the associated plan is independently determined by each point. The maximum EE is provided by M-MMSE, followed by ZF, while the least EE is produced by MR, as can be shown. In addition to having the greatest EE, M-MMSE also has the smoothest EE near the ideal. This increases its resistance to a variety of network conditions.

From above figure following results are obtained:

Table 2: EE of different Schemes , with Pilot reuse factor and base station Density

Scheme	(Pilot reuse factor ζ , BS Density λ)	EE (Mbit/Joule)
M-MMSE	(3,6)	11.2
ZF	(2,5)	9.63
MR	(2,7)	6.47

Following conclusions are obtained:

- Regardless of the combining structure, the optimum energy efficiency is obtained for a pilot reuse component around 2 or 3 and also for a slightly small base station concentration (less base stations per km^2).
- This is contrast to single slope framework, wherein EE monotonically grows as λ (BS Density) grows.

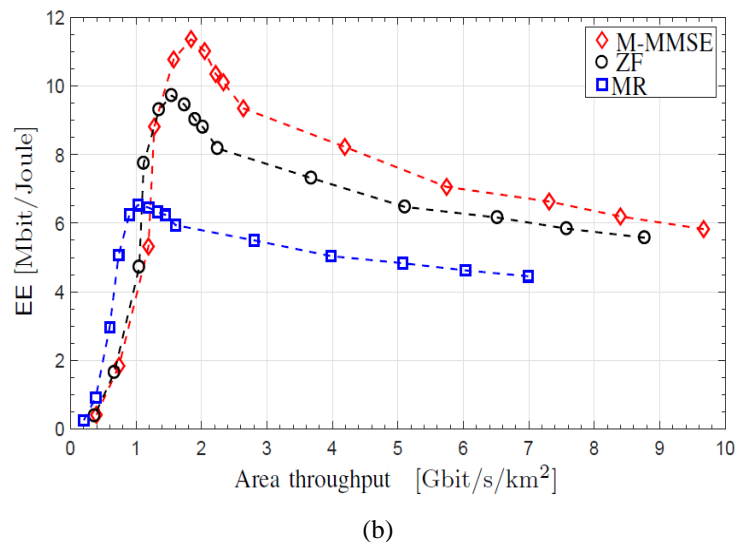
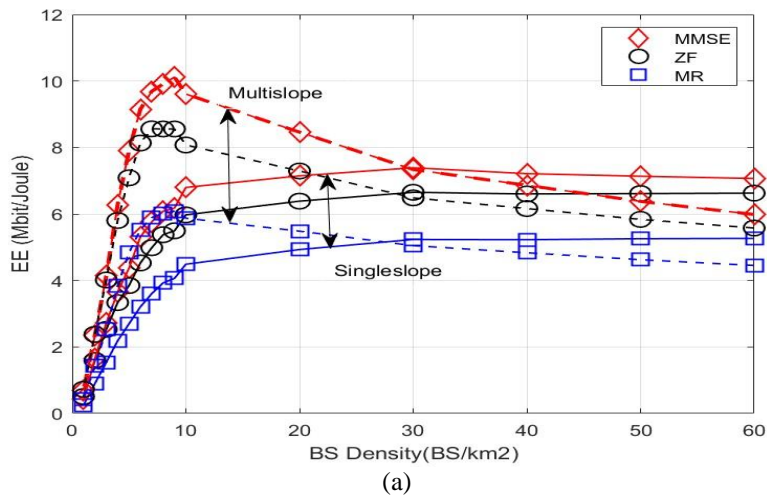


Fig. 3: EE as an assignment of (a) λ (in BS/km²) and (b) Area Throughput in (in Gbit/s/km²). (3a), both single-slope and multi-slope path loss framework are considered. (3b) only the multi-slope is taken. Following results are obtained from figure 3 and are compared with existing literature:

Table 3: Comparison of (a) EE and (b) Throughput for Single slope and Multi slope Pathloss Models

Scheme	Single-slope (EE Mbit/Joule) [18]	Multi-slope (EE Mbit/Joule) (Proposed algorithm)
M-MMSE	7.33	10.124
ZF	6.6	8.55
MR	5.23	6.02

(a)

Scheme	Single-slope (Throughput) [20]	Multi-slope (proposed algorithm)

M-MMSE	11	11.9
ZF	9.6	10
MR	5.07	6.23

(b)

Following conclusions are drawn from obtained results:

- There exist operating where there is a joint increase of each the area throughput and energy efficiency up to the utmost energy efficiency point, but more increase in throughput can only come at a loss in energy efficiency.
- In all schemes, there is a reduction of EE in order to achieve higher throughput.
- Figure 3 shows that the additional dynamic complication of M-MMSE structure pays off twain in terms of energy efficiency and area throughput.

Up to the maximum EE point, it is feasible to boost both the area throughput and energy efficiency simultaneously, however, additional increases in throughput can only result in a reduction in energy efficiency. There are many throughput numbers or, equivalently, base station solidity that yield almost maximum energy efficiency with larger area throughput since the curves are relatively flat near the utmost energy efficiency point.

VIII. Conclusion

In the premise of odd CSI and a multislope path loss framework, a cell web with utmost energy efficiency with MR, ZF, and M-MMSE is constructed. By utilising a lower bound on the SE and a cutting-edge power utilization framework, this was presented as an optimization issue. For a Massive MIMO network, the factors were the pilot reuse component and BS density. The results shown that M-MMSE processing's increased computational complexity pays off in terms of energy efficiency and area throughput, despite the fact that all schemes perform similarly with respect to, i.e., shrinking the cell size has no positive effects on EE.

IX. References

- [1] T. Cisco, 'Cisco Visual Networking Index : Global Mobile Data Traffic Forecast Update , 2014 – 2019', pp. 2014–2019, 2019.
- [2] A. Gupta, S. Member, R. K. Jha, and S. Member, 'A Survey of 5G Network : Architecture and Emerging Technologies', *IEEE Access*, vol. 3, pp. 1206–1232, 2015, doi: 10.1109/ACCESS.2015.2461602.
- [3] A. Fehske, A. Gmbh, and J. Malmudin, 'The Global Footprint of Mobile Communications : The Ecological and Economic Perspective', no. May 2014, 2011, doi: 10.1109/MCOM.2011.5978416.
- [4] N. Bhushan *et al.*, 'Network Densification : The Dominant Theme for Wireless Evolution into 5G', no. February, pp. 82–89, 2014.
- [5] H. S. Dhillon, S. Member, M. Kountouris, and J. G. Andrews, 'Downlink MIMO HetNets : Modeling , Ordering Results and Performance Analysis', vol. 12, no. 10, pp. 5208–5222, 2013.
- [6] J. Hoydis, M. Kobayashi, and M. Debbah, 'Green small-cell networks', *IEEE Veh. Technol. Mag.*, vol. 6, no. 1, pp. 37–43, 2011, doi: 10.1109/MVT.2010.939904.
- [7] Y. S. Soh, S. Member, T. Q. S. Quek, and S. Member, 'Energy Ef fi cient Heterogeneous Cellular Networks', vol. 31, no. 5, pp. 840–850, 2013.
- [8] O. In, 'Seven Ways that HetNets Are a Cellular Paradigm Shift', no. March, pp. 136–144, 2013.
- [9] T. L. Marzetta, 'Noncooperative cellular wireless with unlimited numbers of base station antennas', *IEEE Trans. Wirel. Commun.*, vol. 9, no. 11, pp. 3590–3600, 2010, doi: 10.1109/TWC.2010.092810.091092.
- [10] H. Q. Ngo, E. G. Larsson, and T. L. Marzetta, 'Energy and Spectral Efficiency of Very Large Multiuser MIMO Systems', pp. 1–31, 2011.
- [11] E. Björnson, J. Hoydis, L. Sanguinetti, and E. Bj, 'Massive MIMO Has Unlimited Capacity Massive MIMO Has Unlimited Capacity', 2018.
- [12] A. D. Wyner, 'Shannon-Theoretic Approach to a Gaussian Cellular Multiple-Access Channel', vol. 40, no. 6, pp. 1713–1727, 1994.
- [13] O. Somekh, S. Member, and S. S. Shitz, 'Shannon-Theoretic Approach to a Gaussian Cellular Multiple-

- Access Channel with Fading’, vol. 46, no. 4, pp. 1401–1425, 2000.
- [14] J. G. Andrews, F. Baccelli, and R. K. Ganti, ‘A tractable approach to coverage and rate in cellular networks’, *IEEE Trans. Commun.*, vol. 59, no. 11, pp. 3122–3134, 2011, doi: 10.1109/TCOMM.2011.100411.100541.
- [15] H. S. Dhillon, S. Member, and R. K. Ganti, ‘Modeling and Analysis of K -Tier Downlink Heterogeneous Cellular Networks’, pp. 1–11.
- [16] D. Cao, S. Zhou, and Z. Niu, ‘Optimal Base Station Density for Energy-Efficient Heterogeneous Cellular Networks’, pp. 4379–4383, 2012.
- [17] S. Cho and W. Choi, ‘Energy-Ef fi cient Repulsive Cell Activation for’, vol. 31, no. 5, pp. 870–882, 2013.
- [18] E. Bj, ‘Deploying Dense Networks for Maximal Energy Efficiency : Small Cells Meet Massive MIMO’, pp. 1–15.
- [19] D. Tse, ‘Fundamentals of Wireless Communication 1’, 2004.
- [20] X. Wang, *Massive MIMO Networks : Spectral , Energy , and Hardware Efficiency*.
- [21] A. Pizzo, D. Verenzuela, L. Sanguinetti, and E. Bj, ‘Network Deployment for Maximal Energy Efficiency in Uplink with Zero-Forcing’, 2017.
- [22] E. Björnson *et al.*, ‘Optimal Design of Energy-Efficient Multi-User MIMO Systems : Is Massive MIMO the Answer ? To cite this version : HAL Id : hal-01242459 Optimal Design of Energy-Efficient Multi-User MIMO Systems : Is Massive MIMO the Answer ?’, 2015.
- [23] H. Q. Ngo, A. Ashikhmin, H. Yang, E. G. Larsson, and T. L. Marzetta, ‘Cell-Free Massive MIMO versus Small Cells’, vol. 16, pp. 1834–1850, 2017.
- [24] X. Zhang and J. G. Andrews, ‘Downlink Cellular Network Analysis with Multi-slope Path Loss Models’, pp. 1–14, 2015.